Simple UV-Grafting of PolyAcrylic and PolyMethacrylic Acid on Silicone Breast Implant Surfaces: Chemical and Mechanical Characterizations

Anna Wozniak, Vincent Humblot, Romain Vayron, Rémi Delille, Celine Falentin-Daudre

Simple UV-Grafting of PolyAcrylic and PolyMethacrylic Acid on Silicone Breast Implant Surfaces: Chemical and Mechanical Characterizations

Anna Wozniak [1], Vincent Humblot [2], Romain Vayron [3], Rémi Delille [3] and Céline Falentin-Daudré [1,*]

[1] LBPS/CSPBAT, UMR CNRS 7244, Institut Galilée, Université Sorbonne Paris Nord, 99 avenue J.B. Clément, 93430 Villetaneuse, France; anna.wozniak@univ-paris13.fr

[2] Université Franche-Comté, UMR CNRS 6174, Institut FEMTO-ST, 15B avenue des Montboucons, 25030 Besançon, France,; vincent.humblot@femto-st.fr

[3] LAMIH, UMR CNRS 8201, Université Polytechnique Hauts-De-France, 59300 Valenciennes, France;
romain.vayron@uphf.fr (R.V.); remi.delille@uphf.fr (R.D.)

* Correspondence: falentin-daudre@univ-paris13.fr

Abstract: Poly(dimethyl siloxane) (PDMS) is one of the most widely used materials in the biomedical field. Despite its numerous advantages, its hydrophobic character promotes bacterial adhesion and biofilm formation. For breast implants, biocompatibility is challenged due to the biofilm formed around the implant that can degenerate to severe capsular contracture over time. Thus, the laboratory has set up strategies to prevent bacterial contamination by grafting covalently hydrophilic bioactive polymers on the surface of implants. In this study, poly(methacrylic acid) (PMAc) and poly(acrylic acid) (PAAc) were chosen as non-toxic and biocompatible bioactive polymers known for reducing bacteria adhesion. These polymers are also good candidates to lend reactivity on the surface for further functionalization. X-ray photoelectron Spectroscopy (XPS) and Fourier-Transform Infrared spectroscopy (FTIR) analysis have highlighted the covalent grafting of these polymers. Apparent water contact angle measurements have shown the change in hydrophilicity on the surface, and a colorimetric assay allowed us to assess the grafting rate of PMAc and PAAc. Tensile strength assays were performed to ensure that the functionalization process does not significantly alter the material's mechanical properties. Analyses of the surface aspect and roughness by Scanning Electron Microscope (SEM) and optical profilometer allow us to formulate hypotheses to approach the understanding of the behavior of the polymer once grafted.

Keywords: silicone; grafting; biomaterial; implant; bioactive polymer; surface functionalization; mechanical properties

1. Introduction

Polydimethysiloxane (PDMS) is the most widely used silicone for medical applications (medical devices, and implants) thanks to its numerous advantages such as biocompatibility, elasticity, transparency or cost [1–6]. Despite this, inevitable side effects are observed in the medical field [7]. The silicone breast implant represents an interesting case because it is one of the most implanted medical devices [7,8] pointed out by several popular scandals [7] and for its long-term implantation.

When a silicone breast implant is inserted into the body, the immune system responds by forming a fibrous capsule around the implant [9]. It is a natural response called foreign body reaction (FBR) [10]. In some cases, this capsule can contract severely resulting in capsular contracture. This is characterized by the hardening of the fibrous capsule that surrounds the breast implant [11]. This can lead to various symptoms, such as discomfort, deformation and distortion of the implant, and a feeling of stiffness and pain in

the breast area [12]. A surgical removal and replacement of the implant is, therefore, needed. The precise understanding of capsular contracture formation is still unclear, but inflammatory reactions and an excessive immune response at the implant level may contribute to its development [7,13]. Factors such as the patient's genetic predisposition, and the presence of seroma may also play a role [7,14]. As a consequence, the formation of a bacterial biofilm on the surface of the silicone breast implant represents a major infectious problem [11]. Bacterial contamination is linked to the hydrophobic nature of the silicone surface which promotes the adsorption of non-specific plasma proteins which will allow bacterial adhesion and proliferation [15–18]. Bacteria can gain access to the implant surface during implant insertion and through surgical site infections [7,11,12]. Once adhered to the surface, the bacteria will spread and form a protective biofilm [7,11].

Recently, breast implant-associated anaplastic large cell lymphoma (BIA-ALCL), a cancer involving breast implants has been detected in women 8–10 years post-surgery [8,19]. It concerns likely women who have textured implants. Thus, the long-term biocompatibility issue is even more threatened.

Several studies focus on bacterial biofilm formation around implanted medical devices [5,9,10,20–22]; it still represents challenges in terms of understanding and finding appropriate treatment [9,12].

Preventing the capsular contracture and bacterial biofilm formation on these implants appears necessary [11]. Covalent grafting of bioactive polymers [23] with antibacterial or antimicrobial properties on the implant surface represents an attractive solution [24–27]. PDMS can be modified at its surface by grafting macromolecules carrying functional characteristics [28–30]. However, working on PDMS material is still a challenge because of its inert character.

Previous work in our team has focused on the establishment of a covalent grafting of an anionic bioactive polymer carrying sulfonate groups: sodium polystyrene sulfonate (pNaSS) [31]. A 'grafting from' technique through ultraviolet (UV) pre-irradiation is used to create reactive groups on the surface of the initially inert silicone surface [32]. Different characterization techniques allowed us to highlight the covalent grafting of such bioactive polymers, and biological studies can confirm the improvement in biocompatibility by analyzing cell proliferation on the surface [16]. Analyses of the capsular contracture around the explants showed the presence in the vast majority of *Staphylococcus epidermidis* [7,12,33]. The sulfonated polymer has the capacity to modify the organization of certain proteins adhering to the surface which will thus prevent the adhesion of bacteria, but remains ineffective with other proteins involved in the mechanism such as fibrinogen [34,35]. Therefore, the objective is to extend and improve the study of simple grafting on silicone surfaces to other bioactive polymers more suited to breast implant issues.

The following study focuses on the grafting of bioactive polymers bearing carboxylate groups such as polyacrylic acid (PAAc) and methacrylic acid (PMAc) and their chemical and mechanical characterizations. These compounds are chosen as non-toxic, biocompatible and hydrophilic polymers [10,36–42]. These bioactive polymers are also very reactive [43], they have the ability to form strong bonds with various materials and are also used as surgical adhesives [44]. The main advantage given to these bioactive polymers regarding biomedical applications is their anti-adhesive property [38,40,44]. At a physiological pH, PAAc and PMAc are found carrying carboxylate groups [38]. The presence of a negative charge on the surface of the material may create repulsions between a negatively charged surface and the positively charged organisms [37]. This way, carboxylated polymers have the advantage of inhibiting cell adhesion by preventing the adhesion of proteins or by modifying their surface organization [20,33,35,45–47].

Ultimately, polymers such as polyacrylic acid (PAAc) can easily be modified in order to be functionalized with other chemical groups, bioactive molecules, and nanoparticles, to give the polymer specific properties for targeted applications [44]. These advantages make carboxylated polymers solid candidates for preventing capsular contracture but also for other long-term implanted silicone medical devices.

To carry out this work, PolycAcrylic Acid (PAAc) and PolyMethacrylic Acid (PMAc) were grafted onto silicone surfaces according to the method developed in the laboratory [32] using the « grafting from » technique and under UV irradiation. To ensure the covalent nature of the grafting, characterization methods such as apparent contact angle measurement, Fourier-Transform Infrared (FTIR) spectroscopy, X-ray Photoelectron Spectroscopy (XPS) and Toluidine Blue (TB) colorimetric assay are used. This last characterization method will also allow us to evaluate the surface grafting rate. The main purpose of the surface functionalization of silicone is to prevent bacterial problems on the surface. However, the surface chemical change must not alter the mechanical properties of the material. It will, therefore, be essential to compare the mechanical characteristics of the grafted silicone with the non-grafted one. Thus, Scanning Electron Microscopy (SEM) observations will first be carried out to determine if functionalization impacts our surfaces. Then tensile tests will complete the study to determine whether the grafted silicone retains the same mechanical behavior as a non-grafted silicone. Finally, acquisitions with an optical profilometer were performed to observe and formulate hypotheses on the behavior of polymers on the surface: arrangement, homogeneity, and chain spreading. These first chemical and mechanical characterizations will pave the way for future biological and bacterial tests that will determine the biological impact of functionalization.

2. Materials and Methods

2.1. Materials

Silicone samples of 1 × 1 cm were cut from breast implant envelopes from SEBBIN company (France). Samples are washed with distilled water for 24 h and dried in an oven at 37 °C for one night before use.

Acrylic acid (AAc, Sigma-Aldrich, France) and methacrylic acid (MAc, ThermoFisher scientific, France) monomers were purified on a column with an inhibitor remover (Sigma-Aldrich, France).

The bioactive polymer grafting on the silicone surface was performed using a two-step "grafting from" technique (Figure 1).

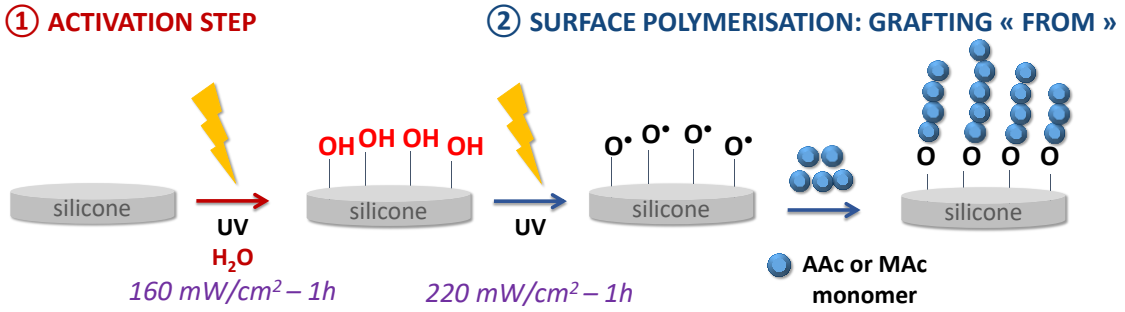

Figure 1. Scheme of the silicone surface grafting.

2.2. Functionalization Process

First step—surface activation: the 1*1 cm PDMS sample is placed in a round-bottom flask containing 60 mL of water and pressed against a Teflon pad hanging from a rod covered with Teflon in order to keep the sample straight. The medium is degassed for 30 min under argon before being placed for one hour in contact with UV radiation from a low-pressure mercury source LOT Oriel (Palaiseau, France) or LED lamp Omnicure (Fast Drying Systems SA, Switzerland) (365 nm) at a power of 160 mW/cm².

Second step—grafting and surface polymerization: still suspended to a Teflon rod, the sample is transferred to a flask containing 60 mL of a 0.35 M monomer solution (MAc or AAc), previously degassed for 30 min under argon. The mixture is then placed 1 h at a power of 220 mW/cm² facing the UV radiation of the Lot Oriel lamp for the grafting in the presence of AAc, and the LED lamp for the MAc grafting.

A grafting condition has been added for AAc in which the pH of the solution containing the monomer is adjusted to pH = 5.25 corresponding to pKa(AAc) + 1. The pH is adjusted with a solution of NaOH in order to obtain a solution containing the monomer with carboxylate groups (AAc-pH).

The samples are then rinsed with distilled water for 48 h to remove the excess polymer and then dried in an oven for 37 °C before being characterized.

Physisorption: Physisorption tests were performed to determine the covalent nature of the surface polymer grafting by the action of our protocol involving UV irradiation. After the first activation step, silicone surfaces were immersed overnight in a solution of MAc and PAAc at the same concentration as the grafting solution (0.35 M) at room temperature. The samples were then washed for 48 h and analyzed by FTIR spectroscopy and apparent water contact angle measurements.

2.3. Surface Characterizations

Water contact angle measurements (WCA), Fourier-transformed infrared spectroscopy (FTIR), colorimetric assay with Toluidine blue (TB) indicator and X-ray photoelectron spectroscopy (XPS) were used to determine the covalent grafting of PAAc and PMAc on PDMS surfaces. Scanning Electron Microscopy (SEM), and an optical profilometer were used to analyze the bioactive polymer behavior on the silicone surface once grafted. Tensile strength tests were performed to verify that the initial mechanical properties of the silicone implant were kept.

Apparent Water Contact Angle Measurement (WCA): After grafting, the wettability of the silicone samples was determined using a KRUSS GmbH DAS10 measuring system (Germany). Three 2 µL drops were deposited on the surface of the samples of each grafting condition. The apparent water contact angle measurement was recorded 10 s after drop deposition with the DSA drop shape analysis software and averages were calculated.

Attenuated Total Reflectance—Fourier-transform infrared spectroscopy (ATR-FTIR): Measurements were performed on the Perkin Elmer Spectrum Two Spectrometer (France) at a resolution of 4 cm^{-1} on a spectral range from 600 to 4000 cm^{-1} (16 scans). The square samples of grafted PDMS were pressed with an equivalent force on the diamond crystal. Spectra obtained from the acquisitions were directly fitted and analyzed.

Grafting rate measurement by Toluidine Blue (TB) colorimetric assays: An aqueous solution of 5.10^{-4} M of dissolved Toluidine Blue dye (TB, Carl Roth, France) was prepared. The latter allows a colorimetric assay by complexation and decomplexation of the anionic groups grafted onto the silicone surfaces. The 1 × 1 cm samples are placed for 6 h at 30 °C with stirring in 5 mL of the TB solution adjusted to pH = 10 so that the cationic groups $N^+(CH_3)_2$ of the dye can complex with the negative charges COO^- of the polymers. The samples were then washed three times for 5 min in a NaOH solution (1.10^{-3} M) to remove the excess of non-complexed TB. Finally, the samples were decomplexed overnight in 10 mL of an aqueous solution of acetic acid (50/50 v/v, Sigma, France) protected from light.

This test is based on the hypothesis of Ikada et al. [48] that one mole of TB complexes with one mole of carboxylate ion (-COO^-). Thus, the absorbance of the decomplexing solution measured by UV-vis spectroscopy (633 nm) allows us to determine the concentration of grafted polymer and so to the grafting rate on silicone surfaces.

X-ray Photoelectron Spectroscopy (XPS): In order to analyze the silicone surface changes after PMAc and PAAc grafting, grafted and non-grafted silicone samples were exposed under ultra-high vacuum (≤10^{-10} Torr) to the electron beam of an Omicron XPS Argus spectrometer (Taunusstein, Germany) equipped with a monochromated AlKα radiation source (hν = 1486.6 eV). Photoelectron emission was analyzed at a takeoff angle of 90°, and at a working power of 300 W.

Spectra were obtained by setting up a 100 eV pass energy for the survey spectrum and a pass energy of 20 eV was chosen for the high-resolution regions. Binding energies were calibrated against the C1s binding energy of aliphatic carbon atoms at 284.8 eV. Element peak intensities were corrected by Scofield factors [49]. Casa XPS v.2.3.15 software (Casa Software Ltd., Bay House, 5 Grosvenor Terrace, Teignmouth, Devon, TQ14 8NE,

United Kingdom) was used to fit the spectra, and the Gaussian/Lorentzian ratio was applied (G/L ratio = 70/30).

For each condition (PDMS, PMAc and PAAc), a set of three different samples were analyzed separately.

Surface topography analyses: Scanning Electron Microscopy (SEM): Bare and grafted PDMS surface images were acquired using a HITACHI TM3000 SEM (Japan), allowing us to analyze the surface topography changes. The SEM detects the secondary electrons and an accelerating voltage between 5 and 10 kV is applied. Images were taken at a magnification of 150 and 3000.

The observation area for the image acquisition was chosen to be as representative as possible of the whole sample. The brightness and contrast parameters were adjusted to observe the images of the different grafted samples. Low magnification observations (×150) allow us to observe the impact of the grafting on the surface as a whole. Observation at higher magnification (×3000) allows us to observe more detail of any surface changes after functionalization.

Optical profilometer: A 3D Optical Profilometer ContourGT-K (Bruker, MA, USA) is used to acquire topography and to evaluate through analysis of the surface roughness, parameters calculated from the topographical data measured by a 3D optical green light Bruker interferometer (Contour GT-K1). The measurements were based on non-contact vertical scanning interferometry (VSI—measurement mode) with a 50× objective lens associated with a 2× numerical magnification. The vertical resolution with this technique was approximately 10 nm. A contactless characterization was chosen because of the relatively soft sample surface. For each sample, 10 topographic measurements of 20 μm*20 μm were realized and rugosity parameters were calculated by using Mountains® software (DigitalSurf).

Tensile strength assays: Four dog bone shaped tensile specimens of each type were cut in silicone envelopes and grafted in the center area of interest (2 cm) for non-grafted silicones, PAAc, and PAAc-pH grafted silicones. The samples were maintained by their extremities and tensile strength assays were conducted with an ElectroPuls E3000 electromagnetic machine (Instron, Norwood, MA, USA) in a closed capsule at 37 °C. Black and white paint were sprayed on the area of interest (middle of the specimen) to allow the deformation following (50 mm/min, 2 images/s), then the samples are placed one by one in the test cell at 37 °C to perform. The results obtained were then analyzed with Matlab (Mathworks).

3. Results and Discussion

3.1. Direct Grafting of PMAc and PAAc

The first part of the study focuses on the characterization of the covalent grafting of PMAc and PAAc on the surface.

In previous studies conducted by the laboratory [32], the "grafting from" technique has been effective for the covalent grafting of polymer chains onto PDMS and will thus be used in this study. Other simple techniques are efficient in coating PDMS and improve its properties like layer-by-layer polyelectrolyte deposition [50,51], or one-step painting coatings that can provide direct efficient bactericidal or bacteriostatic effects on materials [52]. However, these techniques do not provide covalent grafting. Here, the "grafting from" technique is attractive because it is conducted in distilled water and does not need specific reagents or temperature conditions, the grafting can be distributed on the surface, and covalent. That makes it suitable for biomedical applications.

The method consists of growing polymer chains from radical species present on the silicone surface. In the first step of the grafting, the silicone sample is exposed to UV irradiation aims to make the initially inert surface reactive. Activation under UV irradiation in water will act on the methyl bonds (*Si-CH*$_3$) of the PDMS present at 785 cm^{-1} on the FTIR spectra (Figure 2). The irradiation will break homolytically the *CH*$_2$*-H* bonds to create hydroxyl (*-OH*) groups on the surface (Figure 1—Step 1). The formation of these groups on the surface can be justified by the presence of ether bonds (*C-O-C*) on the FTIR spectra at

1162 cm^{-1} (Figure 2) formed after the polymerization step (Step 2) between the activated surface and the polymer.

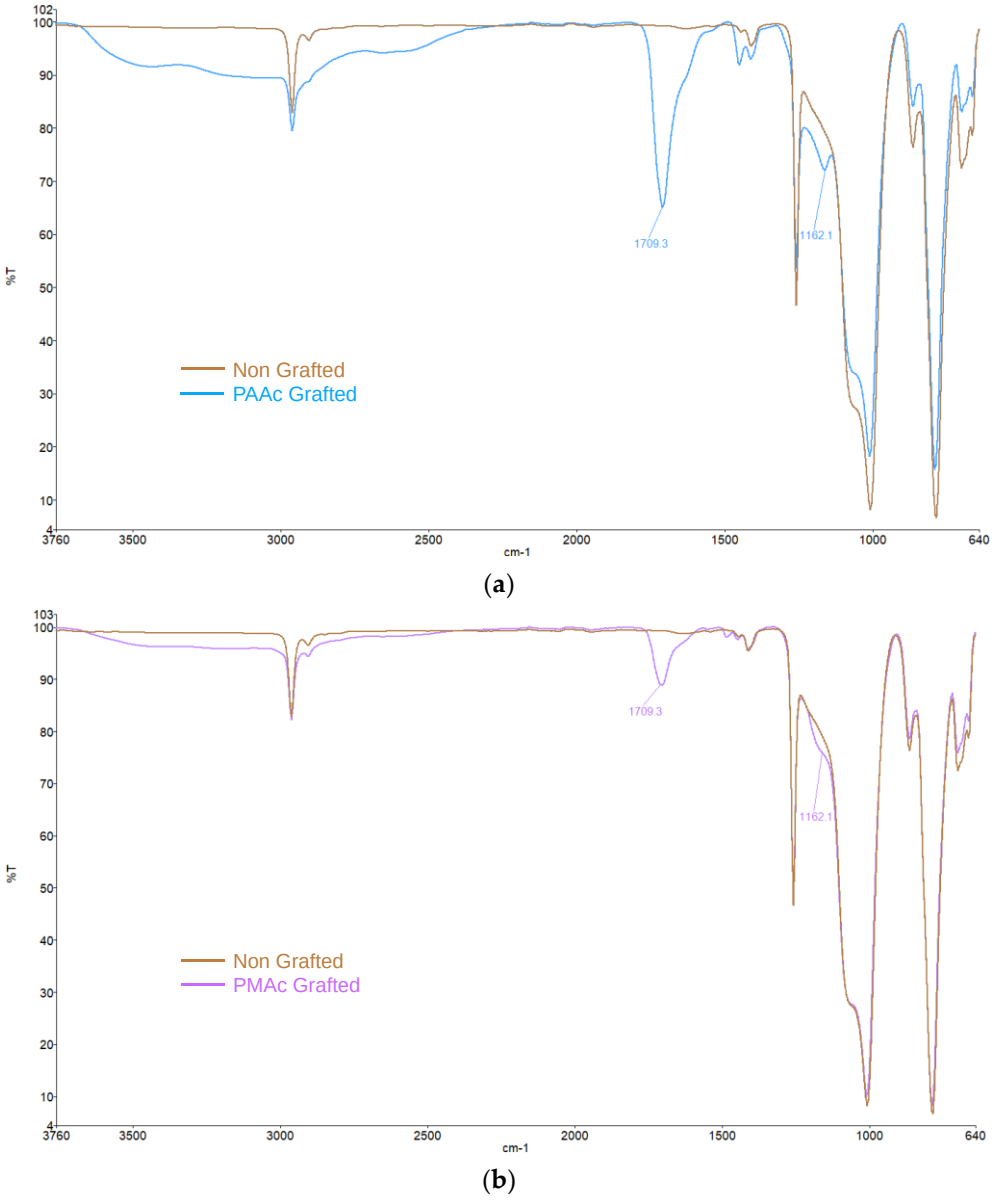

Figure 2. FTIR spectra of (**a**) Non-grafted silicone and PAAc grafted silicone; (**b**) Non-grafted silicone and PMAc grafted silicone.

The following propagation step (Figure 1—Step 2) consists of creating -*O*• radicals from the hydroxyl groups formed during the previous step still under UV irradiation. These radicals will thus attack a molecule of monomer present in solution which will itself attack another monomer to thus form a chain of n monomer units.

To characterize the covalent grafting of the bioactive polymers on the surface, the apparent water contact angle measurement gives us a first indication. Bare silicone surfaces are highly hydrophobic due to the presence of methyl groups preventing water penetration in the PDMS matrix. The attachment of PAAc and PMAc holding hydrophilic functional groups will lend wettability to the surfaces. It is confirmed by the apparent contact angle decrease from 115° to 85.3° and 70.5° for PMAc and PAAc, respectively (Figure 3A). The large standard deviation observed for the apparent contact angle of PMAc grafted samples is explained by the lack of repeatability of the experiment. The hypothesis put forward is that the more diffuse light beam of the LED lamp does not generate reactive groups in a systematic and equivalent way on the surface of the transparent silicone.

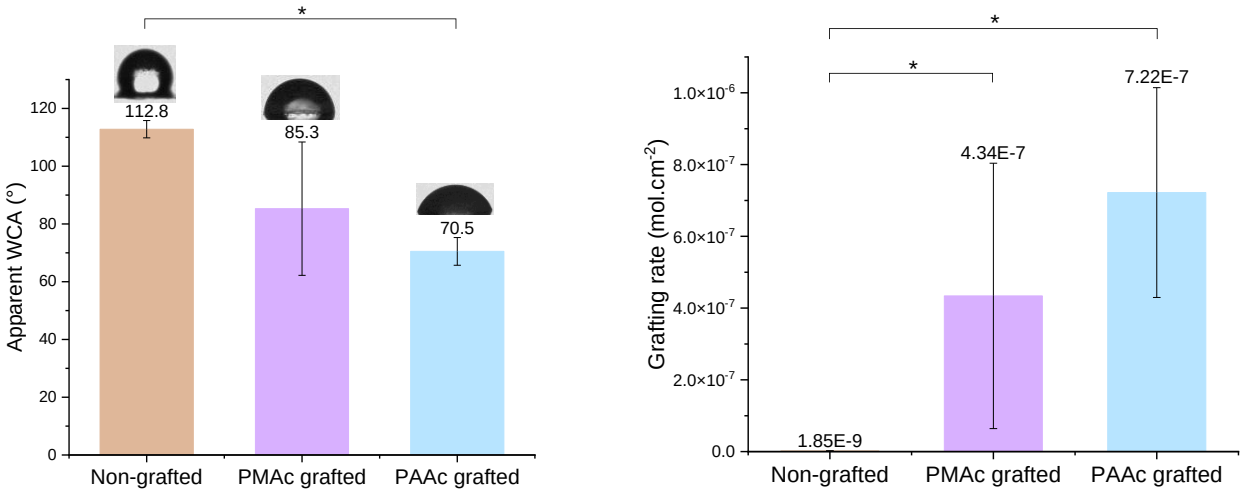

Figure 3. (**a**) Apparent Water Contact Angle (WCA) of non-grafted, PMAc grafted and PAAc grafted silicone; (**b**) Grafting rates of non-grafted, PMAc grafted and PAAc grafted silicone.

X-ray photoelectron spectroscopy assays allow us to work directly on the silicone surface to understand the impact of the functionalization. The atoms composing the two bioactive polymers are already present in the PDMS substrate, namely carbon (C1s) and oxygen (O1s). A non-negligible change can still be noticed by the atomic percentage increase of carbon and oxygen atoms on the surface, and simultaneously a decrease in the silicon atomic percentage (Table 1). These results show first of all the presence of more carbonaceous matter on top of the PDMS substrate, confirmed a second time by the attenuation of the Si2p signal due to energy loss while passing through the organic layer, thus confirming the chemical changes on the surface of the PDMS suggesting the grafting of the PAAc and PMAc.

Table 1. Elementary composition in atomic percentage obtained from XPS analysis of silicone grafted surfaces; means and SD are calculated over 3 separate experiments on 3 separate samples.

Atome	Position * (eV)	%at. Non-Grafted	%at. PMAc Grafted	%at. PAAc Grafted
C1s	283.8	49.1 ± 2.2	54.0 ± 2.3	51.1 ± 2.5
O1s	531.3	23.0 ± 0.3	23.8 ± 0.3	24.4 ± 1.2
Si2p	101.3	27.9 ± 2.1	21.8 ± 2.0	24.5 ± 3.7

* BE for the main feature of the given element.

Moreover, when looking at the high-resolution spectra obtained by XPS on non-grafted PDMS and PAAc and PMAc grafted PDMS, Figure 4, the successful grafting is confirmed. In fact, in the C1s region, two new features appear when compared to bare PDMS. The Binding Energies (BE) observed at 284.4/284.8 eV and 288.3 eV, respectively, in blue and red in Figure 4a are assigned to carbon atoms in C-O and C-Si chemical environment and in C=O, respectively. These are clearly features that would be present in pure PAAc and PMAc films [53]. The same trend is also observed from the O1s region with the appearance of a new feature at higher BE (in red in Figure 4b), also assigned to oxygen in an acidic moiety, namely C-O(C=O). Finally, when looking at the overall atomic percentages for the two grafted PDMS surfaces vs. the bare PDMS surface, Table 2, one can see the great correspondence between the C1s and O1s chemical environments (in red) of the acidic moieties, with 5.6 vs. 5.1 for PAAc and 4.1 vs. 3.9 for PMAc.

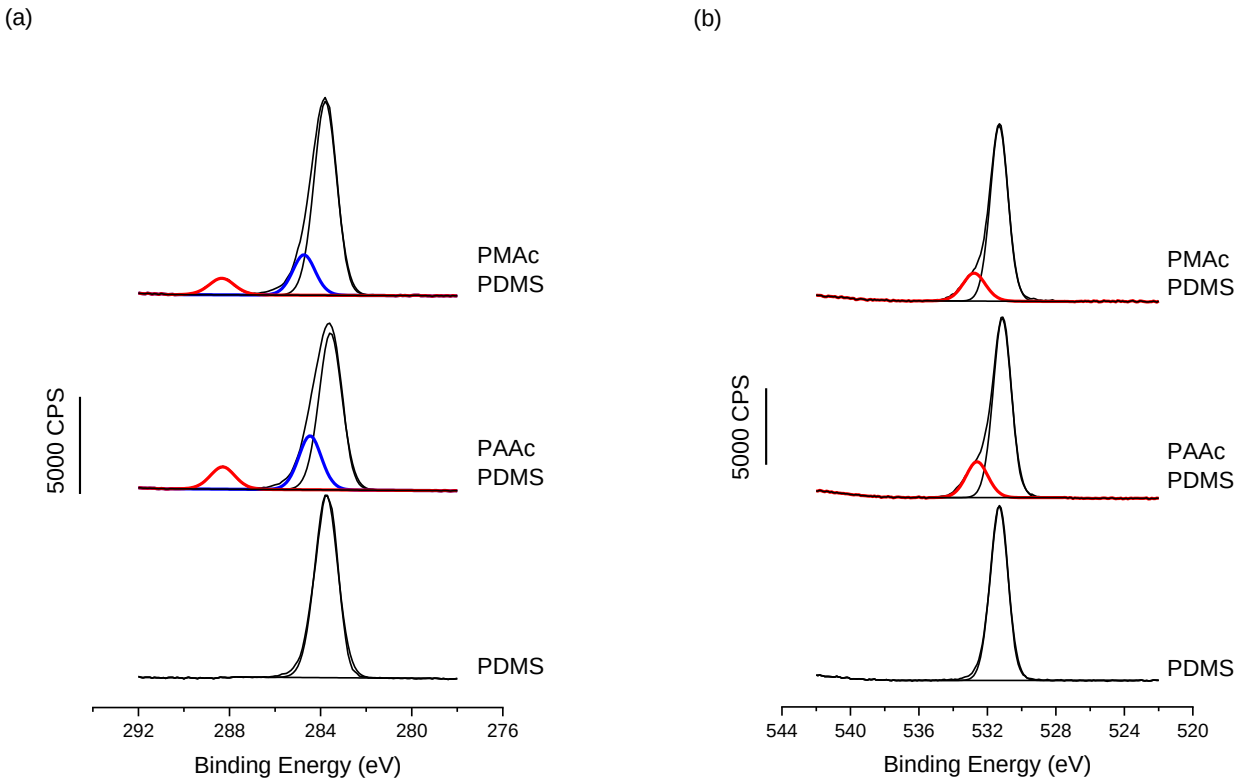

Figure 4. XPS High-Resolution spectra for (**a**) C1s and (**b**) O1s, showing for both PAAc and PMAc the appearance of characteristic features linked to the acrylic moieties, compared to the bare PDMS.

Table 2. Atomic percentages of chemical moiety for each element obtained from decomposition of XPS High-Resolution spectra for C1s and O1s shown in Figure 4.

	C1s			O1s		Si2p	C_{288}/C_{total}	O_{533}/O_{total}
Assignment	**C-C, C-H**	**C-O, Cα**	**C=O**	**C=O(OH) O-Si**	**C=O(OH)**	**Si-O**		
PDMS	**283.8**			**531.3**		**101.2**		
	47.6			22.7		29.7		
PAAc	**283.6**	**284.4**	**288.3**	**531.1**	**532.6**	**101.1**		
	36.25	12.45	**5.6**	20.9	**5.1**	19.8	0.103	0.196
PMAc	**283.8**	**284.8**	**288.3**	**531.3**	**532.8**	**101.3**		
	43.0	9.0	**4.1**	19.5	**3.9**	20.4	0.073	0.166

FTIR spectra allow us to highlight the presence of the characteristic groups bore by the bioactive polymers confirming their presence on the silicone surface. As shown in Figure 2, the characteristic bands of bare silicone correspond to the *Si-O-Si* bonds at 1000 cm^{-1}, 785 cm^{-1} for the *Si-CH₃* bonds as well as a peak at 2962 cm^{-1} corresponding to the *C-H* bonds. These peaks are preserved on all spectra. A clear change is observed after the grafting of polymers with the appearance of a high-intensity peak around 1709 cm^{-1} characteristic of the *C=O* bond. It confirms the presence of the carboxyl group for both graftings. The spectra also show a broad band at 2500–3500 cm^{-1} attributed to the -OH groups of the acid polymers.

TB assays allow us to complete the chemical characterization by evaluating the grafting rates of each bioactive polymer on surfaces. The results presented in Figure 3b show high grafting rates for each condition in comparison to the non-grafted silicone. One can observe that non-grafted silicone already presents a grafting rate. This is due to the non-

specific adhesion of TB on the material. Thus, grafted surfaces must be compared to a control sample to assess whether the grafting rate is notable. Both bioactive polymers have a particularly high rate due to the high reactivity of the monomer and the possible penetration of the polymer into the PDMS matrix [10,37,38]. However, the PMAc-grafted silicone grafting rate shows a high standard deviation. The high reactivity of the monomer and the difficult control of an experiment involving a much more diffusive UV beam could be responsible for the unrepetitive results. Moreover, the wettability results do not always agree with the graft rate values for PMAc grafting. For a given sample, a low apparent contact angle may correspond to a high grafting rate and vice versa. The grafting technique does not allow control over the size of the polymer chains formed on the surface. The high reactivity of PMAc can thus generate long chains of polymer forming a layer on the surface. In this way, the sample, once dried can bring surface irregularities which could explain the low apparent contact angle measurements on a surface associated with a high rate of grafting. Moreover, as observed by Velazco et al. [38] and Yang et al. [37] the polymer could penetrate the silicone matrix and graft inside, limiting surface effects. This hypothesis would explain the change in appearance observed macroscopically on our silicone samples (Figure 6a) and justify the high grafting rate obtained for both polymers. After grafting, the silicone appears hardened and more opaque. The mechanical results discussed later in this study may support these hypotheses. Additional studies on the behavior of the polymer on the surface must be carried out to clarify these variations.

PAAc grafting also presents a high standard deviation. The same hypotheses as the grafting of PMAc can be made regarding the behavior of the polymer at the surface and its penetration in the PDMS matrix. The silicone sample is also harder and more opaque after grafting (Figure 6a). However, the experiment in front of the UV beam remains more repeatable and consistent according to the obtained apparent contact angle values.

At this point, it is worth mentioning that XPS data show the same trend with higher grafting of PAAc than PMAc; indeed, when looking at the ratio of the acidic moieties (C_{288} and O_{533}) in Table 2, normalized by the overall percentages of carbon and oxygen, the PAAc ratio is higher than the PMAc ratio, confirming the higher grafting rate of the first polymer.

Physisorption tests were carried out in order to ensure the covalent nature of the polymers grafting on the surface. The apparent water contact angle measurements show unchanged wettability (Figure 5a), the surfaces remain hydrophobic with an average apparent contact angle of 106° and 103°. FTIR spectra also remain unchanged compared to a non-grafted silicone (Figure 5b). The strong peak characteristic of the *C=O* bond at 1709 cm^{-1} usually present after grafting does not appear. These results highlight the covalent nature of the grafting obtained after the establishment of our protocol.

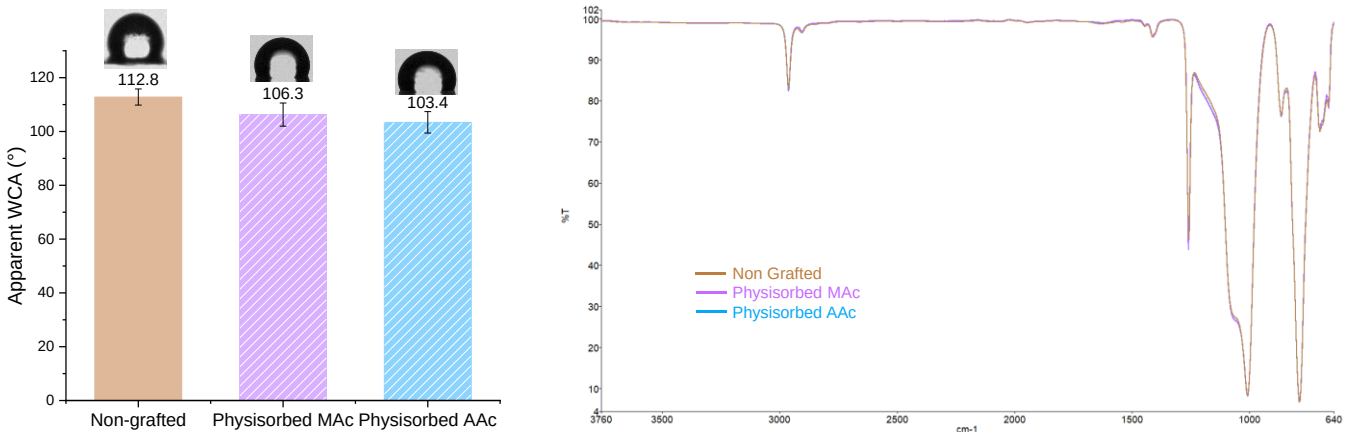

(**a**) (**b**)

Figure 5. (**a**) Apparent WCA of physisorbed polymers; (**b**) FTIR spectra of non-grafted silicone and physisorbed polymers on silicone surface.

The different chemical characterization methods allowed us to highlight the covalent grafting of PMAc and PAAc on the surface of the silicone. However, the significant reactivity of these polymers under the action of UV irradiation generates substantial modifications of the material.

The experiments were carried out with a Lot Oriel mercury source lamp in the case of PAAc grafting which allowed the concentration of the UV beam on the 1*1 cm silicone sample. The grafting of the PMAc was carried out facing an LED lamp whose beam is more diffuse. The grafting of the PMAc facing the concentrated beam of the Lot Oriel lamp damages the surface (hardening, opacification, deformation) (Figure 6a) making it impractical and useless for characterization purposes.

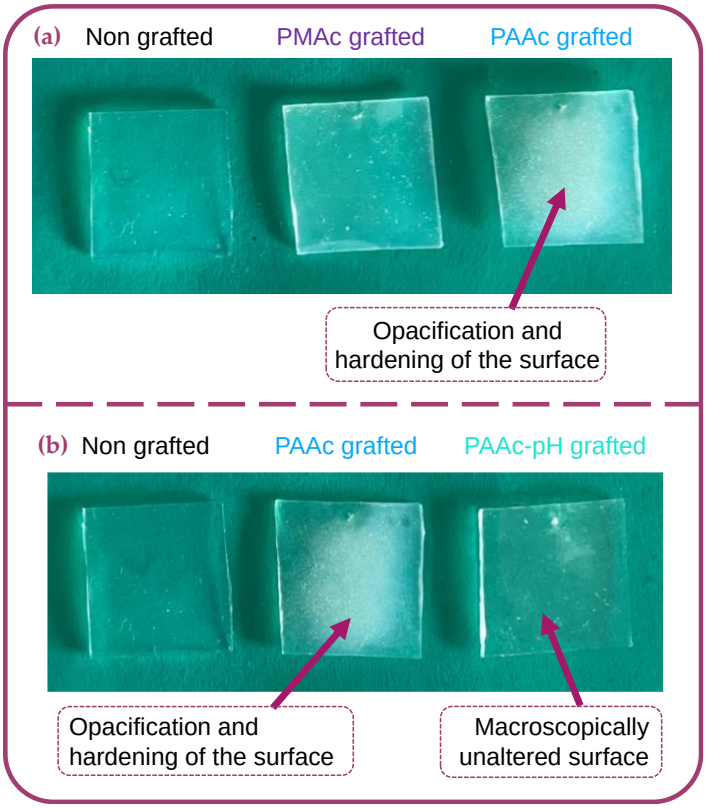

Figure 6. Macroscopical aspect of: (**a**) Bare silicone implant sample, PMAc grafted silicone sample, PAAc grafted silicone sample. (**b**) Bare silicone implant sample, PAAc grafted silicone sample, PAAc-pH grafted silicone sample.

SEM images (Figure 9) were taken to focus on the changes (hardening, opacification) already observed at a macroscopical level on our surfaces (Figure 6a). Figure 9(B1,C1) already shows that at a low magnification of 150, clusters are present on the surface of PMAc and PAAc grafted silicones compared to a bare silicone that appears smooth. (Figure 9(A1)). It is supposed that the large amount of clusters present on the **C1** image compared to the PMAc grafting on the **B1** image is due to the high reactivity of the AAc and the use of the UV lamp with a more concentrated beam. Moreover, by increasing the magnification, we note the change and the significant alteration of the surface of the silicone grafted with PAAc which is completely covered and deformed. The PMAc grafting also shows an alteration of the surface at a magnification of 3000 with the presence of cracks.

In the first part of this study, we were able to highlight the covalent grafting of the two bioactive polymers on the surface. However, a problem of surface alteration remains causing significant unwanted mechanical modifications to the surface particularly impactful for biomedical applications. Thus, the rest of the study will then focus on the grafting adjustment by changing the pH medium condition in order to limit the impact of the acidic polymer. Chemical and mechanical characterization will highlight changes.

3.2. Direct Grafting with pH Middle Adjustment

Due to the uncertain and unrepeatable results of the PMAc grafting, the study chose to only focus on the grafting of the PAAc under new pH adjustment conditions (PAAc-pH). Also, the assays of MAc grafting in the basic medium being inefficient, the condition was not retained for this study.

The same chemical characterizations will make it possible to highlight the covalent character and the grafting efficiency under the new experimental condition. Obtained AAc-pH grafting results are compared with previous direct AAc grafting and non-grafted silicone.

To carry out this part of the study, the « grafting from » technique involving UV irradiations is once again used. The 1*1 cm PDMS samples remain placed in front of the concentrated beam of UV irradiation from the Lot Oriel mercury source lamp for one hour. However, during step 2 of polymerization, the pH of the solution containing the monomer is adjusted with an aqueous NaOH solution to pH = 5.25 corresponding to pKa(AAc) + 1. Thus, the monomer will be present in its basic state carrying carboxylate group COO^- (AAc-pH) in aqueous solution. The duration of this surface polymerization step is still maintained to one hour.

Macroscopically, the silicone surface aspect remains unchanged after grafting in pH-adjusted conditions in comparison to a classic grafting experiment with AAc (Figure 6b). The following chemical surface characterizations will confirm if the bioactive polymer is still covalently grafted on the surface and if differences exist between a PAAc grafted and a PAAc-pH grafted silicone.

Water contact angle measurement shows a similar result as PAAc grafting (Figure 7a). It appears that PAAc-pH grafting on silicone increases the wettability in the same way as PAAc grafting, to an average value of 67°. The repeatability of the experiment is highlighted by a correct standard deviation.

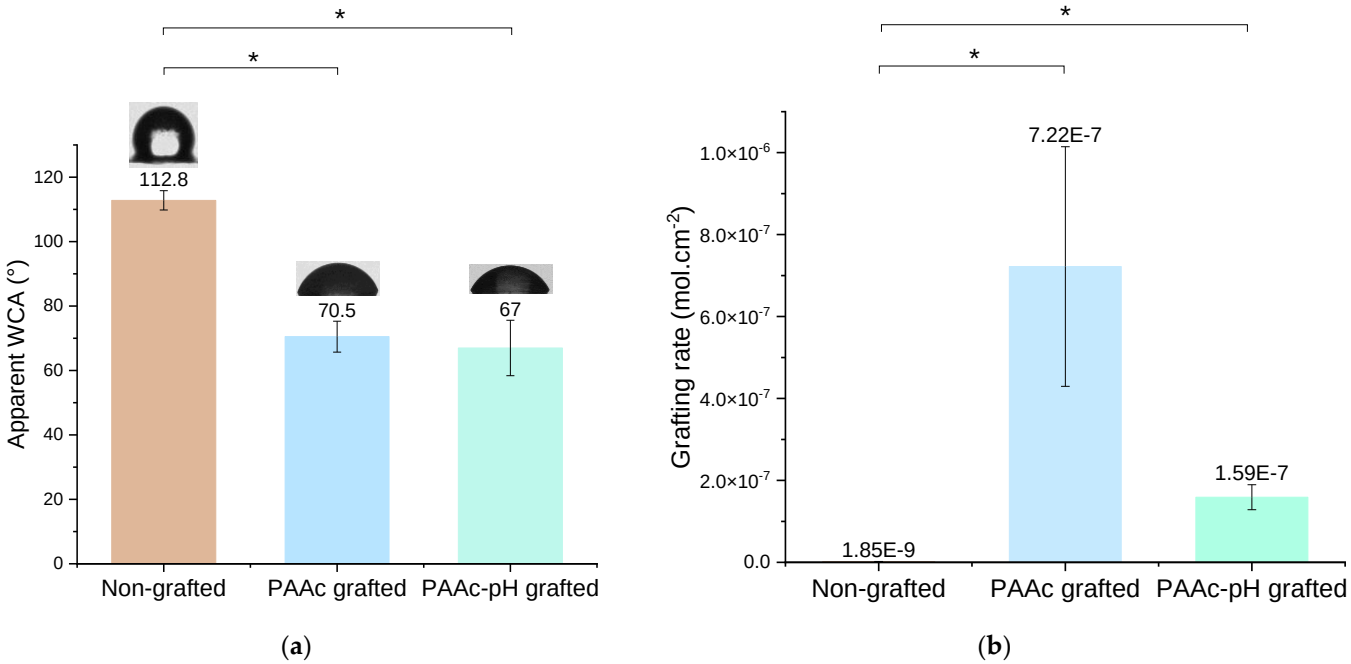

Figure 7. (**a**) Apparent Water Contact Angle (WCA) of non-grafted, PAAc grafted and PAAc-pH grafted silicone; (**b**) Grafting rates of non-grafted, PAAc grafted and PAAc-pH grafted silicone.

FTIR spectra of PDMS grafted with PAAc-pH show that characteristic bands and peaks of bare silicone are still present. The spectra find also the same peak for the *C=O* bond around 1709 cm^{-1}, and a large band between 2500 and 3500 cm^{-1} (Figure 8) confirming that the polyacrylic acid polymer is still present at the surface. XPS analysis strengthens the idea of the presence of the polymer on the surface by higher atomic percentage values of carbon and oxygen on the surface and low silica atomic percentage (Table 3).

The atomic percentage values are even a little more impactful than that of PAAc grafted silicone. Yet, the intensity of the FTIR spectra peaks is weaker for PAAc-pH grafting, which may imply a lower level of polymer. The combination of both results in parallel with the macroscopic observation of the grafted sample can reveal that the bioactive polymer would have less penetration in the sample to promote a grafting on the surface of the samples.

Table 3. Elementary composition in atomic percentage obtained from XPS analysis of silicone grafted surfaces; means and SD are calculated over 3 separate experiments on 3 separate samples.

Atome	Position * (eV)	%at. Non Grafted	%at. PAAc Grafted	%at. PAAc-pH Grafted
C1s	283	49.1 ± 2.2	51.1 ± 2.5	52.3 ± 0.9
O1s	531	23.0 ± 0.3	24.4 ± 1.2	28.5 ± 0.3
Si2p	101	27.9 ± 2.1	24.5 ± 3.7	19.2 ± 1.3

* BE for the main feature of the given element.

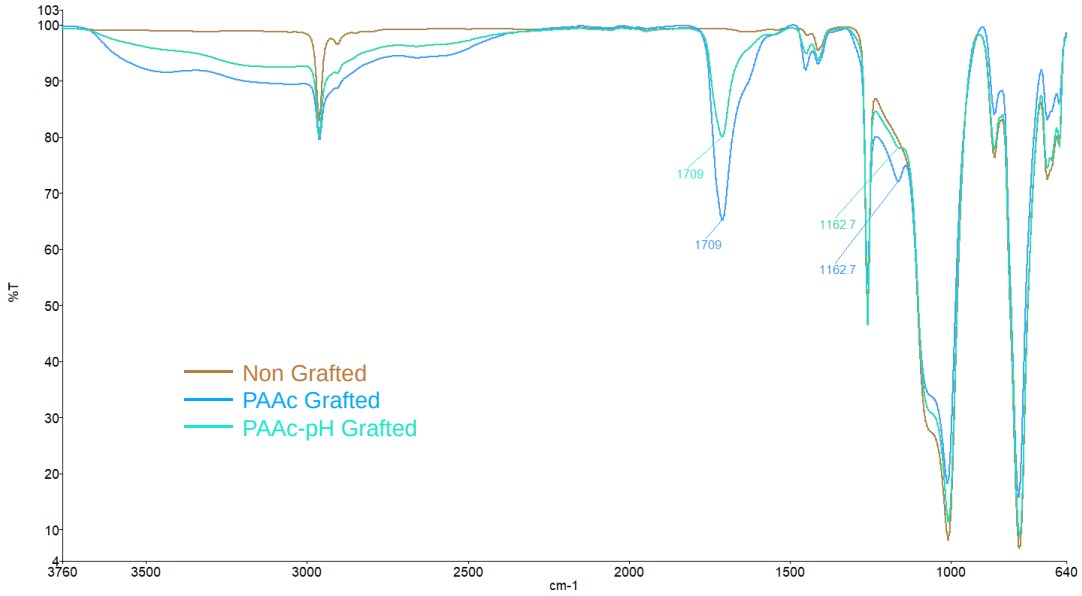

Figure 8. FTIR spectra of non-grafted silicone, PAAc grafted silicone and PAAc-pH grafted silicone.

TB assays allow us to determine the grafting rates of each bioactive polymer on surfaces. The TB assay results presented (Figure 7b) show high grafting rates for each condition in comparison to the non-grafted silicone. PAAc direct grafting has a particularly high grafting rate due to the high reactivity of the monomer and its ability to penetrate the silicone matrix [37,38]. Once grafted with PAAc-pH, the grafting rate became lower than for PAAc due to repulsion between the anionic groups (*COO-*) present in solution and the electrostatic surface of silicone [10]. Thus, less monomer can penetrate the silicone matrix and more grafting occurs on the surface. Even if PAAc-pH grafting appears much lower in comparison to PAAc grafting according to grafting rate value, the bioactive polymer seems to be more present at the surface and the rate could be efficient enough to bring antibacterial effects. According to Lam et al. [16], previous work on sodium polystyrene sulfonate shows that for this polymer, a grafting rate 1 log superior to the control average was enough efficient to allow a performant biological response. Thus, bacterial activity measurement and biological tests must complete this study to go further for medical application purposes.

The surface appearance of the silicone samples observed with the SEM highlights the effect of the grafting of the silicone under the conditions of pH adjustment (Figure 9). The images show that at the microscopic level, the silicone sample is now much less altered than under direct grafting conditions. There are much fewer clusters on surfaces at a magnification of 150 (Figure 9(D1)) and deformities at a magnification of 3000 (Figure 9(D2))

no longer appear. Only a cracking effect persists at the highest magnification, which remains less important than for the PMAc grafting. Thus, we get closer to the initial objective: grafting covalently the surface without modifying the initial mechanical properties of the material.

In the next part of this study, mechanical tensile tests were carried out in order to verify the impact of the different grafting and functionalization protocols on the mechanical properties of the silicone. These results will complete the hypothesis on microscopic observations obtained previously. Surface topography images were also taken with an optical profilometer to find more information about the behavior of the polymers on the surface once grafted using our methods.

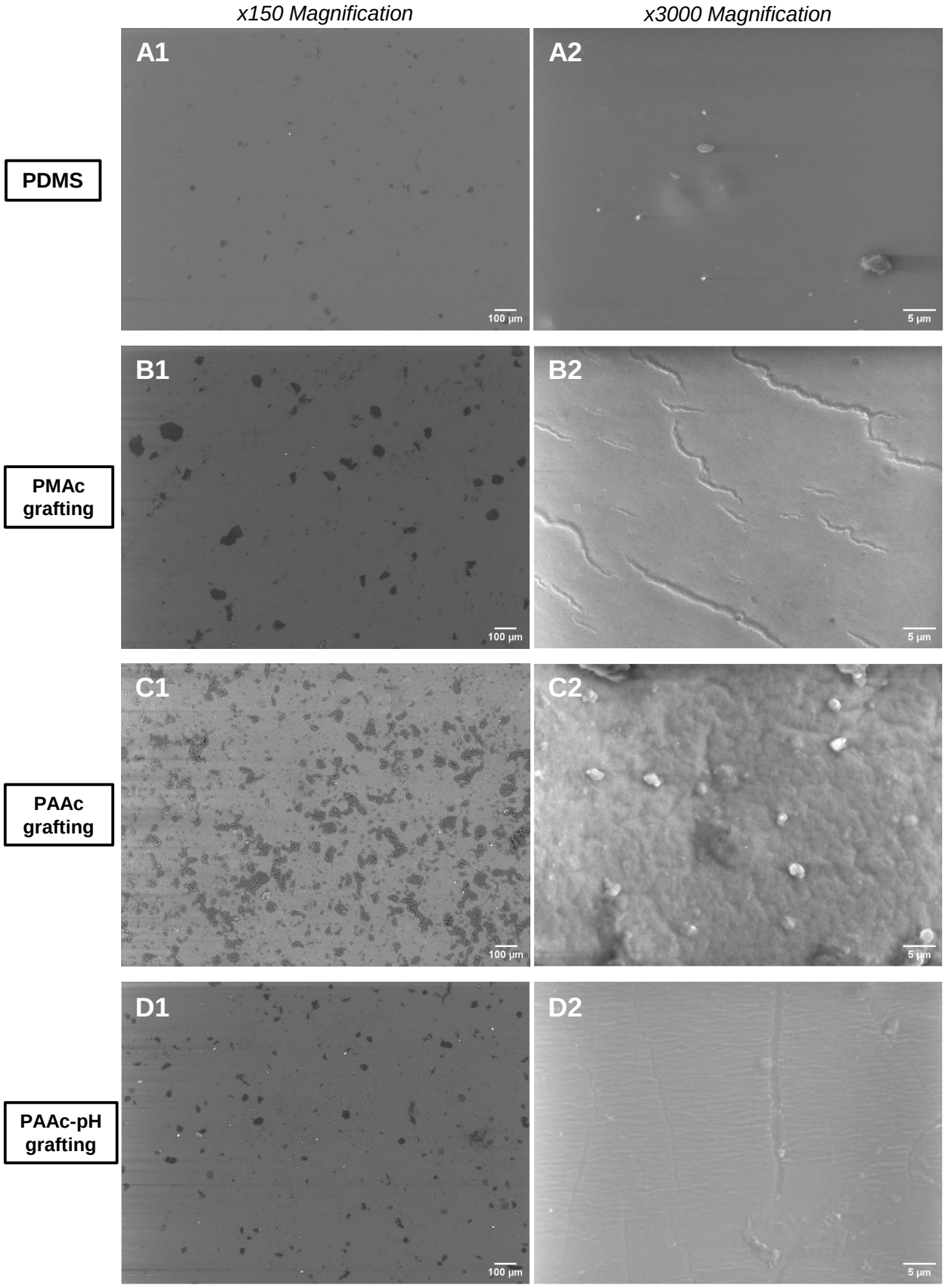

Figure 9. SEM images of: (**A1**) Non-grafted silicone (*150); (**A2**) Non-grafted silicone (*3000); (**B1**) PMAc grafted silicone (*150); (**B2**) PMAc grafted silicone (*3000); (**C1**) PAAc grafted silicone (*150); (**C2**) PAAc grafted silicone (*3000); (**D1**) PAAc-pH grafted silicone (*150); (**D2**) PAAc-pH grafted silicone (*3000).

3.3. Mechanical Assays

Tensile strength tests:

PAAc was directly grafted in an aqueous solution of monomer but also in an aqueous solution with a pH adjusted to the value of pKa(AAc) + 1 = 5.25. This choice was made to counter the enhanced rigidity of the sample obtained with the first grafting condition. Macroscopically, it is already observed that the PDMS has become more rigid, and opaque, and cracks are quickly formed when handling the material. When the pH is adjusted, the PDMS retains its initial appearance at the macroscopic level (Figure 6b). SEM images show that few cracks remain at high magnification (Figure 9(D2)).

The mechanical properties are an essential parameter that appears in the specifications of implantable medical devices. These mechanical properties include the intrinsic properties of the material and the mechanical stress suffered from the action of surrounding tissues and natural movements of life. The silicone envelope is an elastomer. Elastomers are characterized by a low modulus of elasticity meaning that low stress leads to high strain [16]. In this study, tensile tests allowed us to compare the mechanical characteristics of PAAc-grafted silicone under direct grafting conditions and at pH (PAAc-pH) with bare silicone. Lam et al. [16] have already shown that the effect of UV irradiation during the grafting experiment had no significant impact on the mechanical properties of the material. The stress-strain deformation curves are shown in Figure 10 and the obtained Young modulus are summarized in Table 4 and Figure 10. These tests were performed following the ISO 37:2017 or ASTM D412-16 standards [54]. It shows that PAAc-pH grafting does not have a significant impact on the mechanical properties of the material, whose behavior remains close to the ungrafted condition. In comparison, the direct grafting of PAAc shows a significant deviation from the initial conditions.

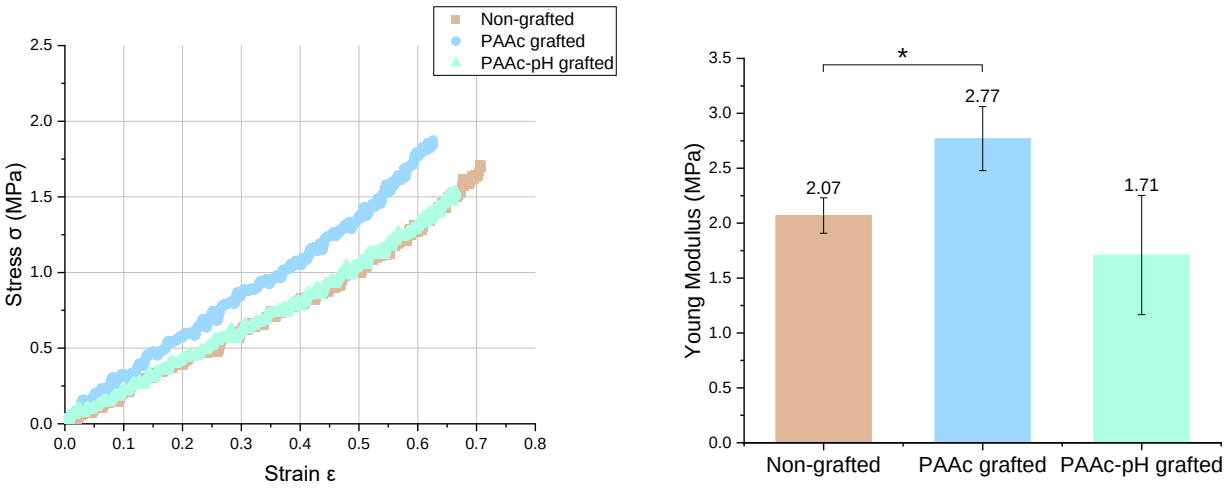

(**a**) (**b**)

Figure 10. (**a**) Stress = f (Strain) curve and (**b**) Young Modulus of non-grafted, PAAc grafted and PAAc-pH grafted silicone samples.

Table 4. Young Modulus value of non grafted, PAAc grafted and PAAc-pH grafted silicones.

	Non-Grafted	**PAAc Grafted**	**PAAc-pH Grafted**
Young modulus (MPa)	2.07 ± 0.16	2.77 ± 0.29	1.71 ± 0.54

Surface topography—Optical profilometer:

Several topographic images were taken on our grafted samples (Figure 11). These acquisitions aim to obtain more information on the behavior of the polymer once grafted on the surface. Figure 11 has been drawn using a color palette optimized for each surface, to better visualize the appearance of the surface rather than its relative height. Yang *et. al*

[37] showed that when PAAc is grafted on PDMS films, the monomers can penetrate and polymerize in the PDMS network, making the material rigid and even brittle. Cracks that appear on the surface offer new interfaces for grafting to other monomers still present in the solution. We have observed this effect with our strategy of direct grafting of the PAAc on the surface. Later, this effect was limited by the presence of COO^- anionic groups during PAAc-pH grafting which generates chain-chain repulsions and silicone surface-chain repulsions [38]. In Figure 11A,C, representing direct grafting of AAc and MAc, the images expose the high reactivity of the polymers and their invasion on the material compared to the surface of non-grafted silicone Figure 11D. Globally, we can highlight the fact that the polymer is present homogeneously on all surfaces. For PAAc-pH grafting (Figure 11B), the polymer behavior seems close to an ungrafted surface. The level of polymers present on the surface seems to be lower. These results correlate with the grafting rate level which appears lower than for a PAAc grafting, but still higher than a non-grafted PDMS (Figure 7b), and with the tensile strength tests where the PAAc-pH samples curve and the Young's Modulus were close to a non-grafted PDMS sample (Figure 10). Actually, there are probably less grafted PAAc on the PAAc-pH grafted samples than for PAAc grafted samples because the grafting occurs mainly on the surface for PAAc-pH. These results remain qualitative, we can also hypothesize that because direct PAAc grafting is reactive it generates many long chains of polymers, while grafting in a basic medium (PAAc-pH) allows the grafting of possibly shorter distributed chains. Now further investigations especially biological assays must complete the study in order to evaluate the efficiency and the effect of the grafting.

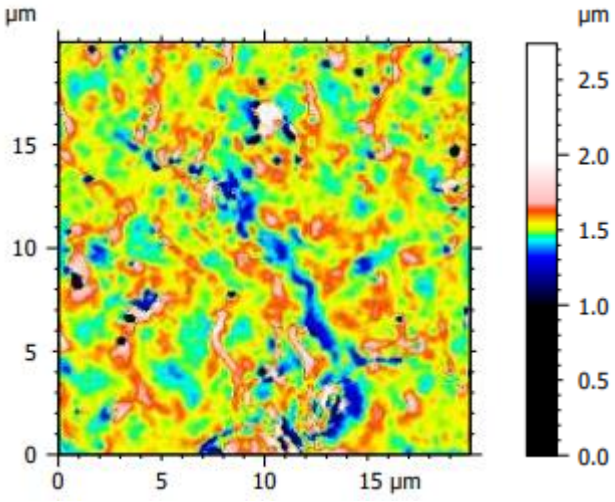

(**A**) PAAc-grafted

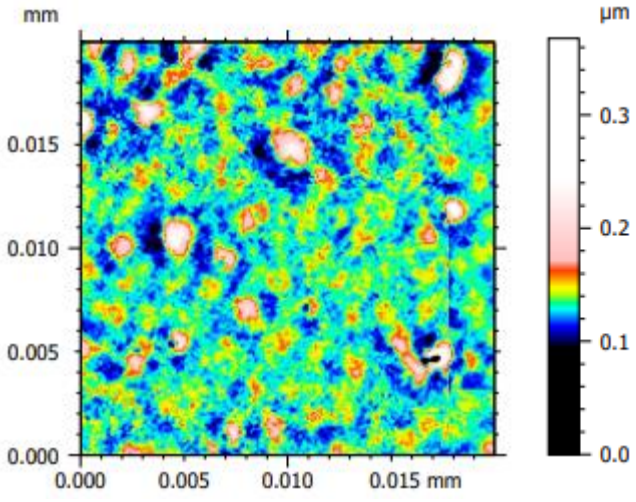

(**B**) PAAc-pH grafted

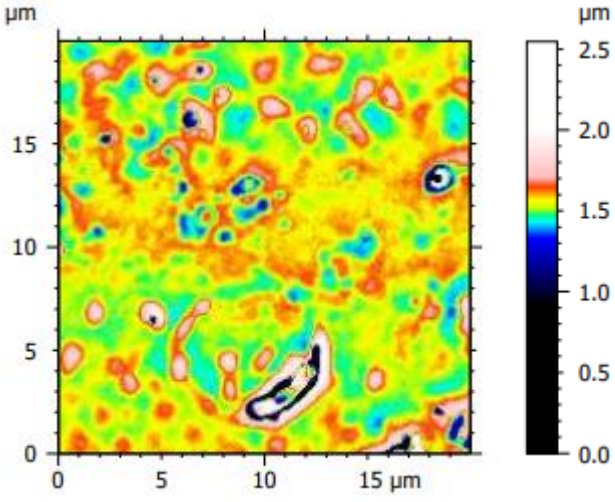

(**C**) PMAc grafted

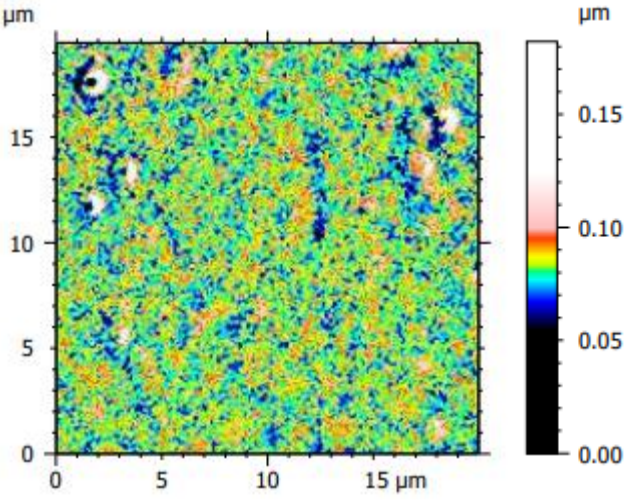

(**D**) Non-grafted

Figure 11. Surface topography of grafted and non-grafted silicone surfaces.

The acquisition of these images also allows us to find the arithmetic heights average (Figure 12). The results show that, on average, the PAAc-pH grafting generates a lower surface roughness close to a non-grafted silicone surface.

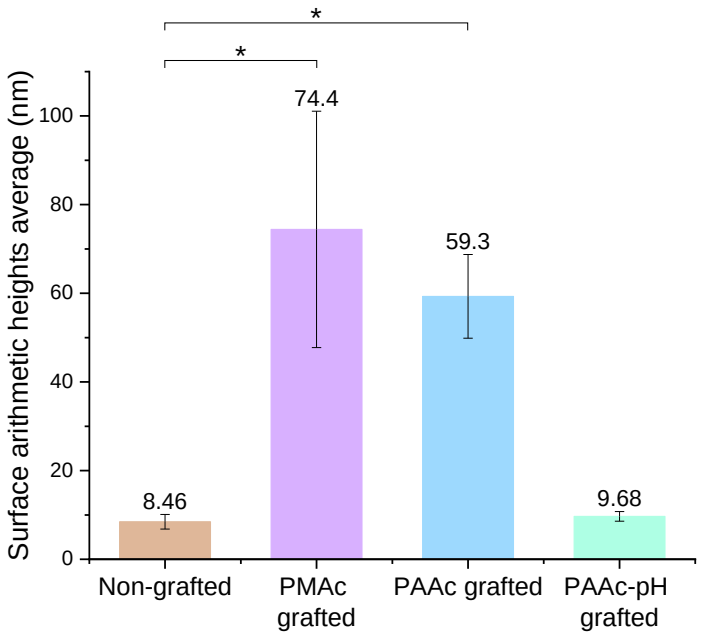

Figure 12. Surface roughness—arithmetic height averages of non-grafted and grafted silicones.

These hypotheses remain to be confirmed by other characterization methods analyzing the behavior of polymers. Note that these measurements were carried out on one sample of each condition because of the soft and electrostatic nature of silicone making difficult the acquisition of topographic images.

4. Conclusions

The study has successfully highlighted that acrylic acid and methacrylic acid can be easily grafted onto silicone using the "grafting from" method with UV irradiation. The increased wettability, the presence of characteristic acid bonds on FTIR spectra, the atomic modifications on the surface and the evaluation of the grafting rate have revealed the covalent nature of this grafting. However, the direct grafting of these polymers promoted their penetration into the PDMS and thus generated modifications of the material such as its hardening and opacification increasing its fragility.

This issue has been limited by adapting the grafting protocol. By adjusting the pH of the medium, the monomer in solution was present in its basic state generating repulsive interactions between the monomer and the material. These effects limited the penetration of the polymer which was thus mainly grafted on the surface. Tensile tests have checked that the impact of surface grafting does not significantly change the mechanical properties of the material. These mechanical assays have determined the preferential use of a pH-controlled way of grafting in order to keep the mechanical properties of our silicone material.

These results are promising and encouraging. Biological and bacterial assays are under investigation to specify the antiadhesive and antibacterial properties of PMAc and PAAc once grafted. Moreover, the presence of carboxylic groups in these bioactive polymers will allow the surface to be functionalized with other bioactive molecules, growth factors, nanoparticles, and peptides for further biomedical applications.

Author Contributions: Conceptualization, A.W.; Methodology, A.W. and C.F.-D.; Validation, C.F.-D.; Formal analysis, A.W., V.H., R.V. and R.D.; Investigation, A.W. and C.F.-D.; Resources, R.V.; Writing—original draft, A.W.; Writing—review and editing, V.H. and C.F.-D.; Supervision, C.F.-D. All authors have read and agreed to the published version of the manuscript.

Funding: This research received no external funding.

Informed Consent Statement: Not applicable.

Informed Consent Statement:

Data Availability Statement:

Acknowledgments: This research was supported by the French Ministry of National Education, Higher Education, and Research. The authors also acknowledge IMPC from Sorbonne University (Institut des Mat´eriaux de Paris Centre, FR CNRS 2482) and the C'Nano projects of the Region Ile-de-France, for Omicron XPS apparatus funding.

Conflicts of Interest: The authors declare no conflict of interest.

References

1. Mata, A.; Fleischman, A.J.; Roy, S. Characterization of Polydimethylsiloxane (PDMS) Properties for Biomedical Micro/Nanosystems. *Biomed. Microdevices* **2005**, *7*, 281–293. https://doi.org/10.1007/s10544-005-6070-2.
2. Gonzalez, G.; Chiappone, A.; Dietliker, K.; Pirri, C.F.; Roppolo, I. Fabrication and Functionalization of 3D Printed Polydimethylsiloxane-Based Microfluidic Devices Obtained through Digital Light Processing. *Adv. Mater. Technol.* **2020**, *5*, 2000374. https://doi.org/10.1002/admt.202000374.
3. Abbasi, F.; Mirzadeh, H.; Katbab, A.-A. Modification of Polysiloxane Polymers for Biomedical Applications: A Review. *Polym. Int.* **2001**, *50*, 1279–1287. https://doi.org/10.1002/pi.783.
4. Wolf, M.P.; Salieb-Beugelaar, G.B.; Hunziker, P. PDMS with Designer Functionalities—Properties, Modifications Strategies, and Applications. *Prog. Polym. Sci.* **2018**, *83*, 97–134. https://doi.org/10.1016/j.progpolymsci.2018.06.001.
5. Gayani, B.; Dilhari, A.; Kottegoda, N.; Ratnaweera, D.R.; Weerasekera, M.M. Reduced Crystalline Biofilm Formation on Superhydrophobic Silicone Urinary Catheter Materials. *ACS Omega* **2021**, *6*, 11488–11496. https://doi.org/10.1021/acsomega.1c00560.
6. Dardouri, M.; Bettencourt, A.; Martin, V.; Carvalho, F.A.; Santos, C.; Monge, N.; Santos, N.C.; Fernandes, M.H.; Gomes, P.S.; Ribeiro, I.A.C. Using Plasma-Mediated Covalent Functionalization of Rhamnolipids on Polydimethylsiloxane towards the Antimicrobial Improvement of Catheter Surfaces. *Biomater. Adv.* **2022**, *134*, 112563. https://doi.org/10.1016/j.msec.2021.112563.
7. Lam, M.; Migonney, V.; Falentin-Daudre, C. Review of Silicone Surface Modification Techniques and Coatings for Antibacterial/Antimicrobial Applications to Improve Breast Implant Surfaces. *Acta Biomater.* **2021**, *121*, 68–88. https://doi.org/10.1016/j.actbio.2020.11.020.
8. Marra, A.; Viale, G.; Pileri, S.A.; Pravettoni, G.; Viale, G.; De Lorenzi, F.; Nolè, F.; Veronesi, P.; Curigliano, G. Breast Implant-Associated Anaplastic Large Cell Lymphoma: A Comprehensive Review. *Cancer Treat. Rev.* **2020**, *84*, 101963. https://doi.org/10.1016/j.ctrv.2020.101963.
9. Moris, V.; Lam, M.; Amoureux, L.; Magallon, A.; Guilloteau, A.; Maldiney, T.; Zwetyenga, N.; Falentin-Daudre, C.; Neuwirth, C. What Is the Best Technic to Dislodge Staphylococcus Epidermidis Biofilm on Medical Implants? *BMC Microbiol.* **2022**, *22*, 192. https://doi.org/10.1186/s12866-022-02606-x.
10. Lee, J.S.; Shin, B.H.; Yoo, B.Y.; Nam, S.; Lee, M.; Choi, J.; Park, H.; Choy, Y.B.; Heo, C.Y.; Koh, W. Modulation of Foreign Body Reaction against PDMS Implant by Grafting Topographically Different Poly(Acrylic Acid) Micropatterns. *Macromol. Biosci.* **2019**, *19*, 1900206. https://doi.org/10.1002/mabi.201900206.
11. Shin, B.H.; Kim, B.H.; Kim, S.; Lee, K.; Choy, Y.B.; Heo, C.Y. Silicone Breast Implant Modification Review: Overcoming Capsular Contracture. *Biomater. Res.* **2018**, *22*, 37. https://doi.org/10.1186/s40824-018-0147-5.
12. Bayston, R. Capsule Formation around Breast Implants. *JPRAS Open* **2022**, *31*, 123–128. https://doi.org/10.1016/j.jpra.2021.11.004.
13. Anderson, J.M.; Rodriguez, A.; Chang, D.T. Foreign Body Reaction to Biomaterials. *Semin. Immunol.* **2008**, *20*, 86–100. https://doi.org/10.1016/j.smim.2007.11.004.
14. Mehta-Shah, N.; Clemens, M.W.; Horwitz, S.M. How I Treat Breast Implant–Associated Anaplastic Large Cell Lymphoma. *Blood* **2018**, *132*, 1889–1898. https://doi.org/10.1182/blood-2018-03-785972.
15. Feng, W.; Zhu, S.; Ishihara, K.; Brash, J.L. Adsorption of Fibrinogen and Lysozyme on Silicon Grafted with Poly(2-Methacryloyloxyethyl Phosphorylcholine) via Surface-Initiated Atom Transfer Radical Polymerization. *Langmuir* **2005**, *21*, 5980–5987. https://doi.org/10.1021/la050277i.
16. Lam, M.; Vayron, R.; Delille, R.; Migonney, V.; Falentin-Daudré, C. Influence of Poly(Styrene Sodium Sulfonate) Grafted Silicone Breast Implant's Surface on the Biological Response and Its Mechanical Properties. *Mater. Today Commun.* **2022**, *31*, 103318. https://doi.org/10.1016/j.mtcomm.2022.103318.
17. Chouirfa, H.; Evans, M.D.M.; Bean, P.; Saleh-Mghir, A.; Crémieux, A.C.; Castner, D.G.; Falentin-Daudré, C.; Migonney, V. Grafting of Bioactive Polymers with Various Architectures: A Versatile Tool for Preparing Antibacterial Infection and Biocompatible Surfaces. *ACS Appl. Mater. Interfaces* **2018**, *10*, 1480–1491. https://doi.org/10.1021/acsami.7b14283.

18. Felgueiras, H.P.; Sommerfeld, S.D.; Murthy, N.S.; Kohn, J.; Migonney, V. Poly(NaSS) Functionalization Modulates the Conformation of Fibronectin and Collagen Type I To Enhance Osteoblastic Cell Attachment onto Ti6Al4V. *Langmuir* **2014**, *30*, 9477–9483. https://doi.org/10.1021/la501862f.
19. Mehdi, A.S.; Bitar, G.; Sharma, R.K.; Iyengar, S.; El-Sharkawi, D.; Tasoulis, M.K.; Attygalle, A.D.; Cunningham, D.; Sharma, B. Breast Implant-Associated Anaplastic Large Cell Lymphoma (BIA-ALCL): A Good Practice Guide, Pictorial Review, and New Perspectives. *Clin. Radiol.* **2022**, *77*, 79–87. https://doi.org/10.1016/j.crad.2021.09.002.
20. Köllnberger, A.; Schrader, R.; Briehn, C.A. Carboxylic Acid Mediated Antimicrobial Activity of Silicone Elastomers. *Mater. Sci. Eng. C* **2020**, *113*, 111001. https://doi.org/10.1016/j.msec.2020.111001.
21. Braem, A.; Kamarudin, N.H.N.; Bhaskar, N.; Hadzhieva, Z.; Mele, A.; Soulié, J.; Linklater, D.P.; Bonilla-Gameros, L.; Boccaccini, A.R.; Roy, I.; et al. Biomaterial Strategies to Combat Implant Infections: New Perspectives to Old Challenges. *Int. Mater. Rev.* **2023**, 1–39. https://doi.org/10.1080/09506608.2023.2193784.
22. Askari, F.; Zandi, M.; Shokrolahi, P.; Tabatabaei, M.H.; Hajirasoliha, E. Reduction in Protein Absorption on Ophthalmic Lenses by PEGDA Bulk Modification of Silicone Acrylate-Based Formulation. *Prog. Biomater.* **2019**, *8*, 169–183. https://doi.org/10.1007/s40204-019-00119-x.
23. Arif, Z.U.; Khalid, M.Y.; Sheikh, M.F.; Zolfagharian, A.; Bodaghi, M. Biopolymeric Sustainable Materials and Their Emerging Applications. *J. Environ. Chem. Eng.* **2022**, *10*, 108159. https://doi.org/10.1016/j.jece.2022.108159.
24. Michiardi, A.; Hélary, G.; Nguyen, P.-C.T.; Gamble, L.J.; Anagnostou, F.; Castner, D.G.; Migonney, V. Bioactive Polymer Grafting onto Titanium Alloy Surfaces. *Acta Biomater.* **2010**, *6*, 667–675. https://doi.org/10.1016/j.actbio.2009.08.043.
25. Pereira, C.; Baumann, J.-S.; Humblot, V.; Falentin-Daudré, C. Biological Properties of Direct Grafting by Ultraviolet Irradiation of Vinyl Benzyl Phosphonic Acid onto Titanium Surfaces. *React. Funct. Polym.* **2022**, *173*, 105215. https://doi.org/10.1016/j.reactfunctpolym.2022.105215.
26. Chouirfa, H.; Migonney, V.; Falentin-Daudré, C. Grafting Bioactive Polymers onto Titanium Implants by UV Irradiation. *RSC Adv.* **2016**, *6*, 13766–13771. https://doi.org/10.1039/C5RA24497H.
27. Amokrane, G.; Falentin-Daudré, C.; Ramtani, S.; Migonney, V. A Simple Method to Functionalize PCL Surface by Grafting Bioactive Polymers Using UV Irradiation. *IRBM* **2018**, *39*, 268–278. https://doi.org/10.1016/j.irbm.2018.07.002.
28. Yammine, P.; Pavon-Djavid, G.; Helary, G.; Migonney, V. Surface Modification of Silicone Intraocular Implants To Inhibit Cell Proliferation. *Biomacromolecules* **2005**, *6*, 2630–2637. https://doi.org/10.1021/bm058010l.
29. Migonney, V.; Lacroix, M.D.; Ratner, B.D.; Jozefowicz, M. Silicone Derivatives for Contact Lenses: Functionalization, Chemical Characterization, and Cell Compatibility Assessment. *J. Biomater. Sci. Polym. Ed.* **1996**, *7*, 265–275. https://doi.org/10.1163/156856295X00300.
30. Crémieux, A.-C.; Pavon-Djavid, G.; Mghir, A.S.; Hélary, G.; Migonney, V. Bioactive Polymers Grafted on Silicone to Prevent Staphylococcus Aureus Prosthesis Adherence: In Vitro and in VIVO Studies. *J. Appl. Biomater. Biomech.* **2003**, *1*, 178–185.
31. Lam, M.; Falentin-Daudré, C. Implication of the Nature and Texturation of Silicone Surfaces on the Grafting of PolyNaSS, a Bioactive Polymer. *IRBM* **2022**, *43*, 687–693. https://doi.org/10.1016/j.irbm.2021.12.003.
32. Lam, M.; Moris, V.; Humblot, V.; Migonney, V.; Falentin-Daudre, C. A Simple Way to Graft a Bioactive Polymer—Polystyrene Sodium Sulfonate on Silicone Surfaces. *Eur. Polym. J.* **2020**, *128*, 109608. https://doi.org/10.1016/j.eurpolymj.2020.109608.
33. Lam, M.; Falentin-Daudré, C. Characterization of Plasmatic Proteins Adsorption on Poly(Styrene Sodium Sulfonate) Functionalized Silicone Surfaces. *Biophys. Chem.* **2022**, *285*, 106804. https://doi.org/10.1016/j.bpc.2022.106804.
34. Vasconcelos, D.M.; Falentin-Daudré, C.; Blanquaert, D.; Thomas, D.; Granja, P.L.; Migonney, V. Role of Protein Environment and Bioactive Polymer Grafting in the S. Epidermidis Response to Titanium Alloy for Biomedical Applications. *Mater. Sci. Eng. C* **2014**, *45*, 176–183. https://doi.org/10.1016/j.msec.2014.08.054.
35. Poussard, L.; Ouédraogo, C.P.; Pavon-Djavid, G.; Migonney, V. Inhibition de l'adhérence de Staphylococcus epidermidis sur des surfaces en titane par des polymères hydrosolubles bioactifs comportant des fonctions sulfonate, phosphate ou carboxylate. *Pathol. Biol.* **2012**, *60*, 84–90. https://doi.org/10.1016/j.patbio.2010.07.004.
36. De Giglio, E.; Cometa, S.; Cioffi, N.; Torsi, L.; Sabbatini, L. Analytical Investigations of Poly(Acrylic Acid) Coatings Electrodeposited on Titanium-Based Implants: A Versatile Approach to Biocompatibility Enhancement. *Anal. Bioanal. Chem.* **2007**, *389*, 2055–2063. https://doi.org/10.1007/s00216-007-1299-7.
37. Yang, H.; Hou, Z. Homogenous Grafted Poly(Acrylic Acid) Brushes on Ultra-Flat Polydimethlysiloxane (PDMS) Films by UV Irradiation. *Nano BioMed. Eng.* **2011**, *3*, 42–46. https://doi.org/10.5101/nbe.v3i1.p42-46.
38. Velazco-Medel, M.A.; Camacho-Cruz, L.A.; Bucio, E. Modification of PDMS with Acrylic Acid and Acrylic Acid/Ethylene Glycol Dimethacrylate by Simultaneous Polymerization Assisted by Gamma Radiation. *Radiat. Phys. Chem.* **2020**, *171*, 108754. https://doi.org/10.1016/j.radphyschem.2020.108754.
39. Schneider, M.H.; Willaime, H.; Tran, Y.; Rezgui, F.; Tabeling, P. Wettability Patterning by UV-Initiated Graft Polymerization of Poly(Acrylic Acid) in Closed Microfluidic Systems of Complex Geometry. *Anal. Chem.* **2010**, *82*, 8848–8855. https://doi.org/10.1021/ac101345m.
40. Zuñiga-Zamorano, I.; Meléndez-Ortiz, H.I.; Costoya, A.; Alvarez-Lorenzo, C.; Concheiro, A.; Bucio, E. Poly(Vinyl Chloride) Catheters Modified with pH-Responsive Poly(Methacrylic Acid) with Affinity for Antimicrobial Agents. *Radiat. Phys. Chem.* **2018**, *142*, 107–114. https://doi.org/10.1016/j.radphyschem.2017.02.008.
41. Ganguly, S.; Maity, P.P.; Mondal, S.; Das, P.; Bhawal, P.; Dhara, S.; Das, N.C. Polysaccharide and Poly(Methacrylic Acid) Based Biodegradable Elastomeric Biocompatible Semi-IPN Hydrogel for Controlled Drug Delivery. *Mater. Sci. Eng. C* **2018**, *92*, 34–51. https://doi.org/10.1016/j.msec.2018.06.034.

42. Liu, Y.; Han, Y.; Wu, Y.; Xiong, L.; Hang, T.; Ling, H.; Hu, A.; Gao, L.; Li, M. Grafting of Poly(Methacrylic Acid-Co-Acrylamide) Film on Silicon Surface via a Simultaneous Hydrolysis Process. *Mater. Today Commun.* **2019**, *21*, 100678. https://doi.org/10.1016/j.mtcomm.2019.100678.
43. Arif, Z.U.; Khalid, M.Y.; Noroozi, R.; Hossain, M.; Shi, H.H.; Tariq, A.; Ramakrishna, S.; Umer, R. Additive Manufacturing of Sustainable Biomaterials for Biomedical Applications. *Asian J. Pharm. Sci.* **2023**, *18*, 100812. https://doi.org/10.1016/j.ajps.2023.100812.
44. Arkaban, H.; Barani, M.; Akbarizadeh, M.R.; Pal Singh Chauhan, N.; Jadoun, S.; Dehghani Soltani, M.; Zarrintaj, P. Polyacrylic Acid Nanoplatforms: Antimicrobial, Tissue Engineering, and Cancer Theranostic Applications. *Polymers* **2022**, *14*, 1259. https://doi.org/10.3390/polym14061259.
45. Chiang, E.N.; Dong, R.; Ober, C.K.; Baird, B.A. Cellular Responses to Patterned Poly(Acrylic Acid) Brushes. *Langmuir* **2011**, *27*, 7016–7023. https://doi.org/10.1021/la200093e.
46. Salloum, D.S.; Schlenoff, J.B. Protein Adsorption Modalities on Polyelectrolyte Multilayers. *Biomacromolecules* **2004**, *5*, 1089–1096. https://doi.org/10.1021/bm034522t.
47. Dai, J.; Baker, G.L.; Bruening, M.L. Use of Porous Membranes Modified with Polyelectrolyte Multilayers as Substrates for Protein Arrays with Low Nonspecific Adsorption. *Anal. Chem.* **2006**, *78*, 135–140. https://doi.org/10.1021/ac0513966.
48. Kato, K.; Ikada, Y. Selective Adsorption of Proteins to Their Ligands Covalently Immobilized onto Microfibers. *Biotechnol. Bioeng.* **1995**, *47*, 557–566. https://doi.org/10.1002/bit.260470508.
49. 1975_Scofield_Hartree-Slater-Subshell-Photoionization-Cross-Sections-At-1254-And-1487-eV.Pdf.
50. Frueh, J.; Gai, M.; Yang, Z.; He, Q. Influence of Polyelectrolyte Multilayer Coating on the Degree and Type of Biofouling in Freshwater Environment. *J. Nanosci. Nanotech.* **2014**, *14*, 4341–4350. https://doi.org/10.1166/jnn.2014.8226.
51. Frueh, J.; Reiter, G.; Möhwald, H.; He, Q.; Krastev, R. Orientation Change of Polyelectrolytes in Linearly Elongated Polyelectrolyte Multilayer Measured by Polarized UV Spectroscopy. *Colloids Surf. A Physicochem. Eng. Asp.* **2012**, *415*, 366–373. https://doi.org/10.1016/j.colsurfa.2012.08.070.
52. Park, D.; Wang, J.; Klibanov, A.M. One-Step, Painting-Like Coating Procedures To Make Surfaces Highly and Permanently Bactericidal. *Biotechnol. Prog.* **2006**, *22*, 584–589. https://doi.org/10.1021/bp0503383.
53. Davies, M.C.; Lynn, R.A.P.; Hearn, J.; Paul, A.J.; Vickerman, J.C.; Watts, J.F. Surface Chemical Characterization Using XPS and ToF-SIMS of Latex Particles Prepared by the Emulsion Copolymerization of Methacrylic Acid and Styrene. *Langmuir* **1996**, *12*, 3866–3875. https://doi.org/10.1021/la960169j.
54. ISO (International Organization for Standardization). Available online: https://www.iso.org/obp/ui/fr/#iso:std:iso:14607:ed-3:v2:en (accessed on October 2022).